RSC Advances

ROYAL SOCIETY OF CHEMISTRY

www.rsc.org/advances

Cite this: DOI: 10.1039/c0xx00000x

www.rsc.org/xxxxxx

ARTICLE TYPE

Up/down conversion tunable photoluminescence and energy transfer properties of $NaLa(WO_4)_2$: Er^{3+}, Eu^{3+} phosphors

Yan Liu, Yanxia Liu, Guixia Liu,* Xiangting Dong and Jinxian Wang

Received (in XXX, XXX) Xth XXXXXXXXX 20XX, Accepted Xth XXXXXXXXX 20XX

DOI: 10.1039/b000000x

Er^{3+} or/and Eu^{3+} codoped $NaLa(WO_4)_2$ down conversion (DC) and up conversion (UC) phosphors were prepared by a facile hydrothermal process. For $NaLa(WO_4)_2$:Er^{3+} phosphors, WO_4^{2-} group can efficiently absorb ultraviolet (UV) light and emit bright blue and green emissions and the f–f transitions of Er^{3+} by the host sensitization effect, respectively. The critical distance of the Er^{3+} ions in $NaLa(WO_4)_2$ is calculated and the energy quenching mechanism is proven to be resonant type dipole–dipole interaction. More significantly, in the Er^{3+} and Eu^{3+} codoped $NaLa(WO_4)_2$ phosphors, the bright green emissions of Er^{3+} ions and the red characteristic emission of Eu^{3+}ions can be observed, the Er^{3+}–Eu^{3+} energy migration has been demonstrated to be a resonant type by a dipole–dipole mechanism. A color-tunable emissions in $NaLa(WO_4)_2$:Er^{3+},Eu^{3+} microcrystals are realized under different UV radiation, and this could make them good candidates to be used as full-color DC phosphors for near UV-LEDs. More functionally, under near infrared (NIR) of 980 nm laser excitation, these phosphors also exhibit intense green and red emissions by the Er^{3+}–Eu^{3+} energy transfer process, which causes the observed UC of Eu^{3+}. The mechanism of UC luminescence is proposed by the observed dependence of integral intensity on the power of the pumping laser.

1 Introduction

Currently, white light-emitting diodes (WLEDs) have brought about a significant revolution in solid-state lighting and display areas owing to their attractive features such as excellent luminescence characteristics, good stability, high luminescence efficiency, long lifetimes, as well as low cost.[1–3] Recently, conventional WLEDs suffer an unsatisfactory high correlated color temperature (CCT≈ 7750 K) and low color-rendering index (CRI≈ 70-80) for room lighting due to the color scarcity of the sufficient red emission.[4, 5] So near ultraviolet/ultraviolet (nUV/UV)-LED chip combined with tri-band, i.e., RGB (red, green and blue) phosphors have been suggested to achieve white light with high CRI and high power output,[6, 7] but the poor luminescence efficiency inescapably impacted by the reabsorption of blue light. In contrast, novel full-color phosphors especially warm-white-emitting phosphors for WLEDs utilizing a single component are expected to avoid such drawbacks, giving rise to the higher quality of white light. Therefore, the design of a single-component full-color or white-light emitting coactivated phosphor is more and more attractive.[7-12]

In consideration of the Eu^{3+} $^5D_0 \rightarrow {}^7F_J$ (J=1, 2, 3, 4) characteristic emissions in the orange-red region respectively, Eu^{3+} ions are expected to possess superior red color, considered as one of the most frequently useful red emitters in rare earth ions doped materials.[13] As an important dopant, Er^{3+} mainly presents high efficiency characteristic emissions between the emitting states $^2H_{11/2}$, $^4S_{3/2}$ and the excited state $^4I_{15/2}$ for giving intense green composition, which overlaps well with the absorption of Eu^{3+} ($^5D_{3,0} \rightarrow {}^7F_0$ transitions),[7, 14] suggesting that Er^{3+} ions can be utilized as donors to sensitize Eu^{3+} acceptors. It is feasible to produce Er^{3+} and Eu^{3+} co-activated phosphors in inorganic host. At the same time, a sensitizer and an activator co-doped into the same host to exhibit efficient full-color and white emitting by energy transfer between sensitizers and activators and the combination of RGB emissions. Remarkably, the Er^{3+} sensitization effect on Eu^{3+} ion DC emission has been only reported in $BaGd_2O_4$:Tm^{3+}/Er^{3+}/Eu^{3+} phosphors, where tunable emissions were obtained for WLEDs as well as field emission displays (FEDs).[7] Nevertheless the mechanism of energy transfer between Er^{3+} and Eu^{3+} has not been analysized yet. For the first time, we established the mechanism of Er^{3+}–Eu^{3+} energy transfer and the possibility of white-light down-conversion (DC) emission from the Er^{3+}/Eu^{3+} codoped $NaLa(WO_4)_2$ phosphors in the present work. For the $NaLa(WO_4)_2$ compound, it belongs to scheelite type $CaWO_4$ structure, adopting tetragonal phase with excellent physical–chemical stability and individual self-activation property from WO_4^{2-} group, so it is considered recently to be an efficient luminescent host candidate.

More functionally, Er^{3+} ions not only present strong absorption in nUV region (365 nm-410 nm) but also could be efficiently pumped by 980 nm near infrared (NIR). Er^{3+} ions served as the first up conversion (UC) rare-earth ions, were widely utilized for the conversion of NIR radiation to visible light.[14-17] In view of the fact that UC emission from Eu^{3+} activated phosphors is not

possible due to the unavailability of energy levels corresponding to suitable near infrared (NIR) excitations, another activator should be indispensably introduced into the system, as sensitizer for exciting Eu^{3+} ions. Furthermore, as an excellent donor, excited Er^{3+} ion could transfer energy to Eu^{3+} ion and sensitize it in UC system. [14, 18-20] Very few reports on Er^{3+}–Eu^{3+} codoped phosphors and glasses have been studied till now, investigated nearly all in Yb^{3+}–Er^{3+}–Eu^{3+} UC systems, where Er^{3+} as the bridging ion for the energy transfer (ET) between Yb^{3+} and Eu^{3+} ions under NIR excitation. [14, 19, 20] In previous reports, the energy transfer (ET) mechanism from Er^{3+} to Eu^{3+} with NIR excitation has been studied in $NaYF_4$,[14] tellurite glasses[18] and Y_2O_3[20], respectively. Multicolor light emissions have been observed from the reported work in Er^{3+}, Eu^{3+} and Yb^{3+} codoped phosphors.

Following this, in this work, we aim to focus our attentions on $NaLa(WO_4)_2$ as a host, Eu^{3+} and Er^{3+} ions as activated ions. The DC and UC properties of Eu^{3+} and Er^{3+} co-doped $NaLa(WO_4)_2$ phosphors with color-tunable emissions are investigated as well as the sensitization effect of Er^{3+}–Eu^{3+} ions.

2 Experimental section

2.1 Materials

Aqueous solutions of $La(NO_3)_3$, $Er(NO_3)_3$ and $Eu(NO_3)_3$ were obtained by dissolving the rare earth oxides La_2O_3, Er_2O_3, Eu_2O_3 (99.99%) in dilute HNO_3 solution (15 mol/L) under heating with agitation in ambient atmosphere. All the other chemicals were of analytic grade and used as received without further purification.

2.2 Preparation

A series of rare earth-doped $NaLa(WO_4)_2$ phosphors were synthesized by a facile hydrothermal process without further sintering treatment. 1.0 mmol of $RE(NO_3)_3$ (including $La(NO_3)_3$, $Er(NO_3)_3$ and $Eu(NO_3)_3$) were added into 100 mL flask. After vigorous stirring for 20 min, 2.0 mmol of $Na_2WO_4{\cdot}2H_2O$ was slowly added dropwise into the above solution. After additional agitation for 30 min, the resultant milky colloidal suspension was transferred to a 50 mL Teflon bottle held in a stainless steel autoclave, and then heated at 180 °C for 20 h. Finally, as the autoclave was naturally cooled to room-temperature, the precipitates were separated by centrifugation at 8000 r/min for 10 min, washed with deionized water and ethanol in sequence each several times, and then dried in air at 60 °C for 12 h.

2.3 Characterization

X-ray diffraction (XRD) was performed with a Rigaku D/max-RA X-ray diffractometer with Cu Kα radiation (λ= 0.15406 nm) and Ni filter, operating at a scanning speed of 10° min^{-1} in the 2θ range from 10 to 90°, 20 mA, 30 kV. The morphology and composition of the samples were observed by a FEI XL-30 field emission scanning electron microscope (FESEM) equipped with an energy-dispersive X-ray spectrometer (EDS). The excitation and emission spectra, and the luminescence decay curves of samples were measured using a HITACHI F-7000 Fluorescence Spectrophotometer equipped with a Xe lamp as the DC excitation source and a power-adjustable laser diode (980 nm, 0-2 W) as the UC pump source, scanning at 1200 nm/min. All of the measurements were performed at room temperature.

3 Results and discussion

3.1 Crystallization behavior and structure

The XRD patterns of $NaLa(WO_4)_2$ phosphors together with the PDF card (No. 79–1119) are given in Fig. 1. All the diffraction peaks of these samples can be exactly indexed to pure tetragonal phase $NaLa(WO_4)_2$ which belongs to $CaWO_4$ type structure and they match well with the standard values of PDF card (No. 79–1119) indicating that the as-prepared phosphors are single phase and the doping ions do not impact significantly on the host structure.

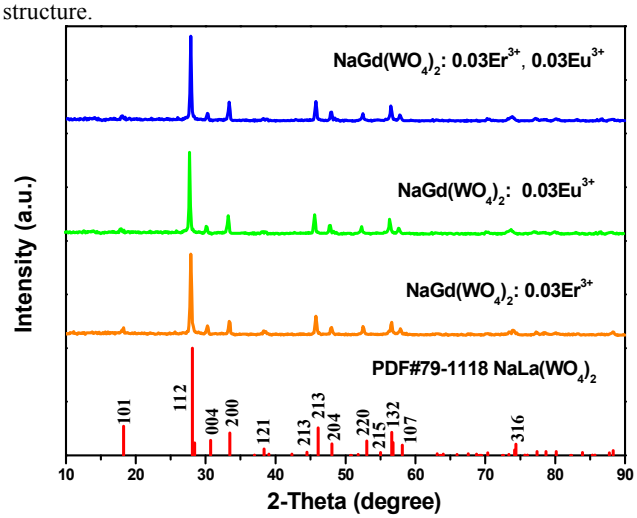

Fig. 1 PDF card (79–1118) and XRD patterns of $NaLa(WO_4)_2$: Er^{3+},Eu^{3+} phosphors

The morphology of $NaLa(WO_4)_2$: Er^{3+}, Eu^{3+} was characterized by FESEM, as presented in Fig. 2a-b. It can be observed that the samples are microparticles composed of many irregular flake-like microcrystals with an average size ranging from 3 to 5 μm. EDS pattern performs the chemical composition of the product, containing Na, La, Er, Eu, W, and O (silicon and chromium signals are from silicon host and spraying chromium process) (shown in Fig. 2c). Combined with above XRD patterns, the samples are further proved to be $NaLa(WO_4)_2$.

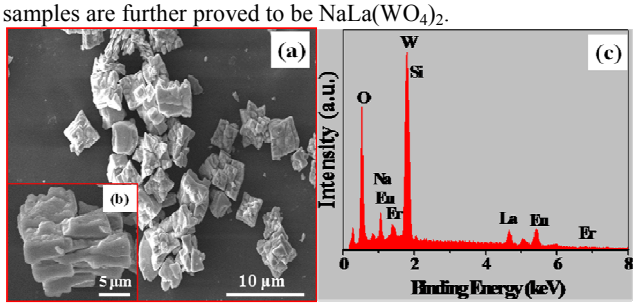

Fig. 2 FESEM images (a, b) and EDS pattern (c) for $NaLa(WO_4)_2$: $0.03Er^{3+}$, $0.03Eu^{3+}$ phosphor

3.2 Down conversion luminescence properties of $NaLa(WO_4)_2$: Er^{3+} phosphors

Fig. 3 illustrates the photoluminescence excitation (PLE) spectrum for $NaLa(WO_4)_2$: $0.03Er^{3+}$. It can be seen that the PLE spectrum consists of two components: the former is a strong and broad band from 200 to 350 nm centered at 285 nm, which can be assigned to the charge transfer (CT) transitions of O^{2-}–W^{6+}

within the WO_4^{2-} groups[21,22], and the latter is the f–f transition of Er^{3+} in the longer wavelength region at 357, 365, 378, 407, 443, 451, 483 nm assigned to the electronic transitions of Er^{3+} ions from the ground level $^4I_{15/2}$ to the $^2G_{7/2}$, $^4G_{9/2}$, $^4G_{11/2}$, $^2H_{9/2}$, $^4F_{3/2}$, $^4F_{5/2}$ and $^4F_{7/2}$ excited levels, respectively. The strongest absorption peak mainly exists at about 378 nm, indicating that the $NaLa(WO_4)_2$: Er^{3+} phosphors could be pumped by nUV used as nUV LED excited phosphors. And the intensity of the peak at 378 nm first increases with the increase of its concentration (x) and reaches a maximum value at x= 0.03 (inset of Fig. 3). The existence of O^{2-}–W^{6+} CT indicates energy transfer from WO_4^{2-} to Er^{3+} in the Er^{3+} ions activated $NaLa(WO_4)_2$ phosphors and Er^{3+} ions could be excited via energy transfer from the WO_4^{2-} groups to the Er^{3+} ions. Therefore, it is a feasible route to realize color-tunable emission in a single host under UV excitation by combining the emissions of the WO_4^{2-} groups and Er^{3+} ions with different Er^{3+} ions doping concentrations.

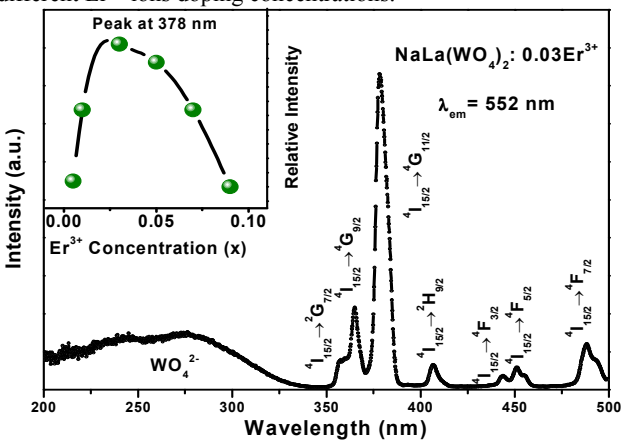

Fig. 3 PLE spectrum for $NaLa(WO_4)_2$: $0.03Er^{3+}$ phosphor (λ_{em}= 552 nm); inset is the dependence of the absorption intensity at 378 nm on different Er^{3+} concentrations

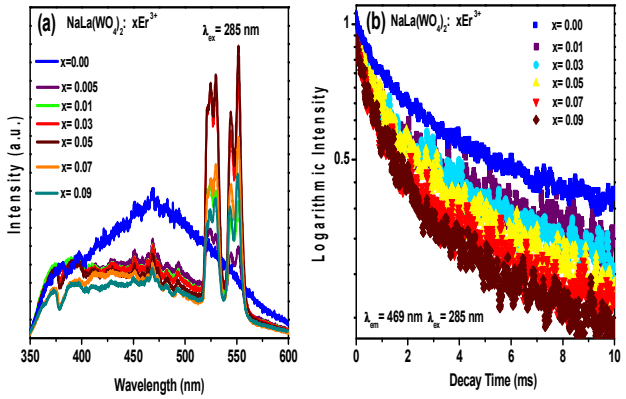

Fig. 4 PL spectra for $NaLa(WO_4)_2$:xEr^{3+} (λ_{ex}= 285 nm) (a) and decay curves for the luminescence of WO_4^{2-} in $NaLa(WO_4)_2$:xEr^{3+} phosphors (excited at 285 nm, monitored at 469 nm) (b)

To further validate the occurrence of the host sensitization effect, the luminescence intensities and the decay times of WO_4^{2-} in $NaLa(WO_4)_2$: xEr^{3+} phosphors with different Er^{3+} concentrations are investigated. Fig. 4a depicts the PL spectra for $NaLa(WO_4)_2$:xEr^{3+} excited by CT transition of O^{2-}–W^{6+} at 285 nm ($^1A_1 \rightarrow {}^1B(^1T_2)$ transition). As revealed, the WO_4^{2-} emission intensity decreases with the increase of Er^{3+}-dopant concentration, accompanied by the enhancement of emission from Er^{3+}, which also supports that there is an energy transfer between Er^{3+} and WO_4^{2-}. Nevertheless not all of the absorption energy of WO_4^{2-} can be transferred to the Er^{3+} ions so that it is noted that upon excitation with 285 nm, $NaLa(WO_4)_2$: $0.03Er^{3+}$ phosphor yields the board blue emission of WO_4^{2-} in short wavelength region and three high intense emission of Er^{3+} in long wavelength region. The decay curves for the luminescence of WO_4^{2-} in $NaLa(WO_4)_2$:xEr^{3+} phosphors excited at 285 nm and monitored at 469 nm are measured and displayed in Fig. 4b. The corresponding luminescent decay curves can be fitted by a single-exponential equation

$$I = I_0 + A\ exp(-t/\tau) \quad (1)$$

On the basic of equation (1), the decay times for WO_4^{2-} are calculated and determined to be 2.5987, 2.3235, 2.1509, 1.9438, 1.9150, 1.7323 ms, respectively. The lifetimes for WO_4^{2-} are found to drastically be decreased with increasing the Er^{3+} concentration.

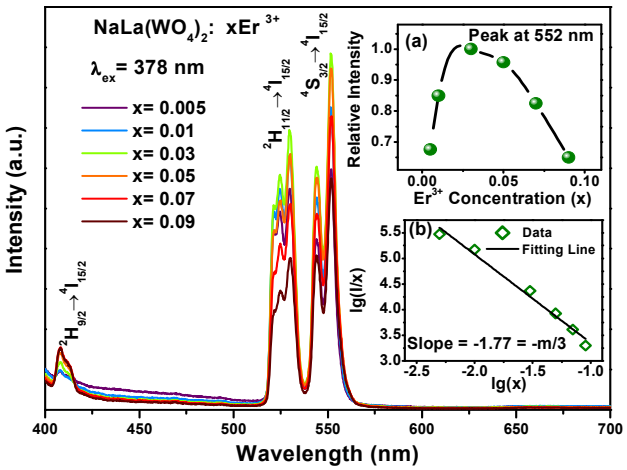

Fig. 5 PL spectra; dependence of relative emission intensity at 552 nm on Er^{3+} concentration (inset, a) and the relationship between Log(I/x) and Log(x) (inset, b) for $NaLa(WO_4)_2$:Er^{3+} phosphors

The PL spectra of $NaLa(WO_4)_2$: xEr^{3+} phosphors are obtained by exciting at 378 nm (Fig. 5). It is noted that $NaLa(WO_4)_2$: xEr^{3+} phosphors give blue and green emissions, corresponding to the $^2H_{9/2} \rightarrow {}^4I_{15/2}$ (408 nm), $^2H_{11/2} \rightarrow {}^4I_{15/2}$ (529 nm) and $^4S_{3/2} \rightarrow {}^4I_{15/2}$ (552 nm) characteristic emissions of Er^{3+} ions, respectively. The strongest one is located at 552 nm ($^4S_{3/2} \rightarrow {}^4I_{15/2}$), which does not change with varying its concentration (x) except for differences in intensity. The optimal Er^{3+}-dopant concentration was found to be 0.03, which is shown in Fig. 5a. With increasing Er^{3+} doping concentration when x< 0.03, the dominating emissions enhance gradually due to the increase of luminescence centers, then decrease when x > 0.03 as a result of the concentration quenching, during which the excitation energy is lost to the killer sites non-radiatively,[23] shown in Fig. 5a. The concentration quenching of the Er^{3+} emission is mainly due to the cross relaxation between neighbouring Er^{3+} ions which are in resonance of their energy levels: Er^{3+} ($^4S_{3/2}$)+ Er^{3+} ($^4I_{15/2}$) →Er^{3+} ($^4I_{9/2}$)+ Er^{3+} ($^4I_{13/2}$).[24]

As an important parameter to evaluate the luminescence properties, the critical distance R_{Er-Er} between Er^{3+} ions can be calculated using the concentration-quenching method [25]

$$R_c = 2\times[3V/(4\pi x_c Z)]^{1/3} \quad (2)$$

where V is the volume of the unit cell, x is the concentration of Er^{3+}, and Z is the number of available crystallographic sites occupied by the activator ions in the unit cell. For the $NaLa(WO_4)_2$ host lattice, V= 332.7 Å^3 and Z= 4. The critical concentration x_c, at which the luminescence intensity of Er^{3+} is quenched, is 0.03. As a result, the critical distance (R_{Er-Er}) of energy transfer is calculated to be about 17.43 Å. As the enhancement of Er^{3+} concentration, the distance between Er^{3+} ions becomes shorter than 17.43 Å, so the resonant energy transfer occurs between neighboring Er^{3+} ions.

According to Van Uiter's report, the interaction type between sensitizers or between sensitizer and activator can be calculated by the following [26, 27]

$$I/x=k[1+\beta(x)^{m/3}]^{-1} \quad (3)$$

in which x is the activator concentration; I/x is the emission intensity (I) per activator concentration (x); k and β are constants; and when the value of m is 6, 8, or 10, the interaction corresponds to dipole-dipole (d-d), dipole-quadrupole (d-q), or quadrupole-quadrupole (q-q), respectively. From equation (3), it can be found that Log (I/x) acts as a linear function of Log(x) with a slope of –m/3. In order to well understand the energy transfer mechanism, we plotted the Log (I/x) versus Log(x) of Er^{3+} as shown in Fig. 5 (inset b). The result of linear fitting presents that the slope is approximate to be –1.77 for $NaLa(WO_4)_2$: xEr^{3+} samples with x varying from 0.01 to 0.03. Therefore, the calculated values of m is nearly coincident with the conventional value of m= 6, meaning that the dominant interaction mechanism for Er^{3+} quenching in the $NaLa(WO_4)_2$ host is based on the dipole-dipole interaction.

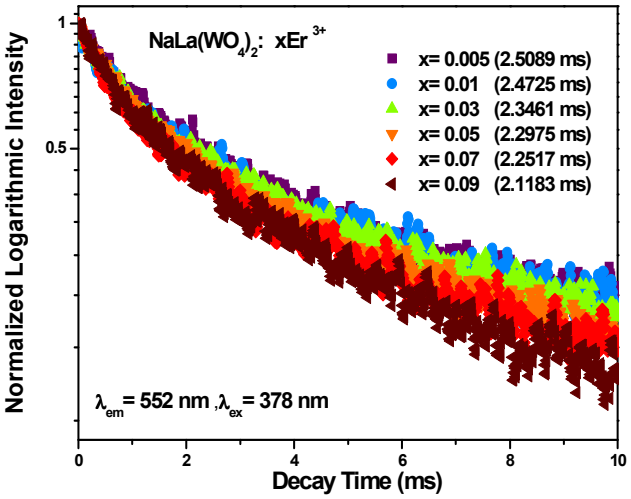

Fig. 6 Decay curves for the luminescence of Er^{3+} ions in $NaLa(WO_4)_2$ phosphors displayed on a logarithmic intensity (excited at 378 nm, monitored at 552 nm)

To further study the luminescence properties of Er^{3+}, the fluorescence decay process of Er^{3+} ions in $NaLa(WO_4)_2$: xEr^{3+} ($0.005\leq x\leq 0.09$) phosphors is investigated by monitored at 552 nm with irradiation of 378 nm. From Fig. 6, one can see that the decay behavior of Er^{3+} can be best fitted to the single-exponential model, employing equation (1), the lifetimes of Er^{3+} ions are determined to be 2.5089, 2.4725, 2.3461, 2.2975, 2.2517 and 2.1183 ms, respectively. The lifetimes for Er^{3+} ions are found to be decreased with increasing Er^{3+} concentration, which is ascribed to the increase of the nonradiative and self-absorption rate of the internal doped ions when activators cross the critical separation between donor and acceptor [28, 29].

3.3 Down conversion luminescence properties of $NaLa(WO_4)_2$: Er^{3+}, Eu^{3+} phosphors and energy transfer between Er^{3+} and Eu^{3+} ions

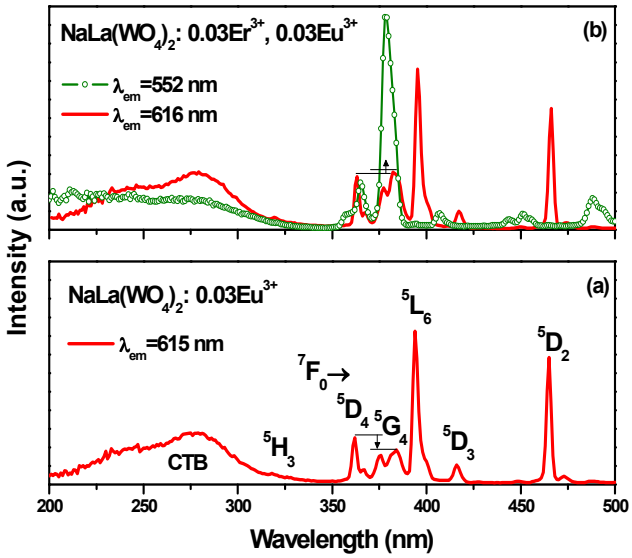

Fig. 7 PLE spectra for $NaLa(WO_4)_2$: $0.03Eu^{3+}$ (a) and $NaLa(WO_4)_2$: $0.03Er^{3+}$,$0.03Eu^{3+}$ (b) phosphors

Fig. 7 shows the PLE spectra for $NaLa(WO_4)_2$:$0.03Eu^{3+}$ (a) and $NaLa(WO_4)_2$:$0.03Er^{3+}$,$0.03Eu^{3+}$ (b) phosphors. In Fig. 7a, the excitation spectrum of $NaLa(WO_4)_2$:$0.03Eu^{3+}$ by monitoring the emission wavelength at 615 nm exhibits some peaks at 323, 364, 385, 395, 416, 466 nm assigned to the transitions of Eu^{3+} ion from the ground level $^7F_0$ to the $^5H_3$, $^5D_4$, $^5L_7$, $^5L_6$, $^5D_3$ and $^5D_2$ excited levels respectively, simultaneously including a broad absorption band in the region 200–350 nm ascribed to CTB of WO_4^{2-} groups and O^2–Eu^{3+} charge transfer transition from an oxygen 2p state excited to an Eu^{3+} 4f state.[11, 13, 30] The f–f transitions of Eu^{3+} from 350 nm to 420 nm match well with the UV-LED chips, indicating that $NaLa(WO_4)_2$:Eu^{3+} are suitable for nUV LED excited phosphors. In Fig. 7b, when monitoring by the green emission of Er^{3+} (552 nm) and red emission of Eu^{3+} (615 nm), the PLE spectra of $NaLa(WO_4)_2$:$0.03Er^{3+}$,$0.03Eu^{3+}$ illustrate some absorption peaks corresponding to the characteristic transitions of Er^{3+} and Eu^{3+}, respectively. More significantly, as shown in Fig. 7b, it can be clearly seen that the excitation spectrum of Eu^{3+} ions at 385 nm in $NaLa(WO_4)_2$: $0.03Er^{3+}$, $0.03Eu^{3+}$ is stronger than that of in $NaLa(WO_4)_2$: $0.03Eu^{3+}$ (Fig.7a) because it consists of typical Er^{3+} and Eu^{3+} f–f excitation bands giving direct evidence to demonstrate the Er^{3+}–Eu^{3+} sensitization effect in the $NaLa(WO_4)_2$ host. Therefore, the tunable color could be generated by combining the green emissions of Er^{3+} ions and red emissions of Eu^{3+} ions via codoping Er^{3+} and Eu^{3+} ions in a single component.

To further elucidate the impact of dopant concentration on the color-tunable emissions in a single component and energy migration process between activators, a series of phosphors fixed Er^{3+} ions concentration were prepared. Fig. 8 illustrates a series of emission spectra for $NaLa(WO_4)_2$:$0.03Er^{3+}$, yEu^{3+} (y= 0.00,

0.005, 0.01, 0.02, 0.025, 0.03, 0.04 and 0.05) under 364 excitation. It can be seen that $NaLa(WO_4)_2$:0.03Er^{3+}, yEu^{3+} phosphors yield the characteristic emissions of both Er^{3+} and Eu^{3+} ions. Fixed the doping concentration of Er^{3+} at 0.03, with increasing Eu^{3+} concentration, the emission intensities of the Eu^{3+} first increase to an optimum concentration at 0.04 then decrease due to the concentration quenching caused by energy transfer between Eu^{3+} luminescent centers, whereas that of the Er^{3+} decreases monotonically, reflecting the result of energy transfer from Er^{3+} to Eu^{3+}. Therefore, the luminescence intensities of various rare-earth ions can be enhanced or quenched by the energy transfer from other codoped rare-earth ions. Those illustrate the occurrence of energy transfer from Er^{3+} to Eu^{3+} when they are codoped in the $NaLa(WO_4)_2$ host and they are provided a necessary condition for synthesizing the single phase full-color phosphors.

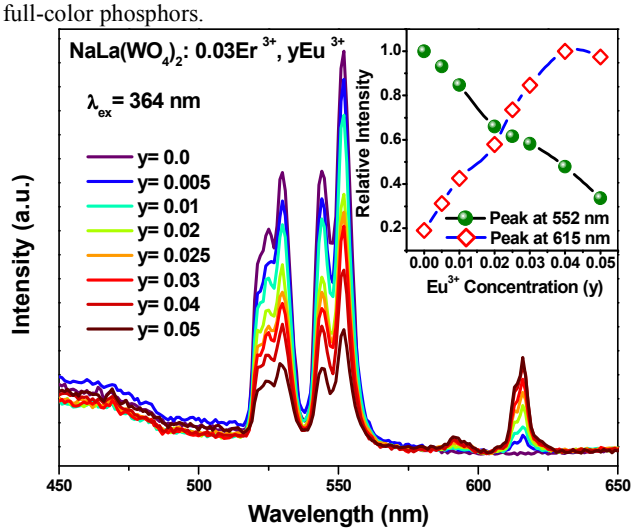

Fig. 8 PL spectra for $NaLa(WO_4)_2$:Er^{3+}, Eu^{3+} phosphors (λ_{ex}= 364 nm); dependence of the absorption intensity at different wavelengths on Eu^{3+} concentrations (inset)

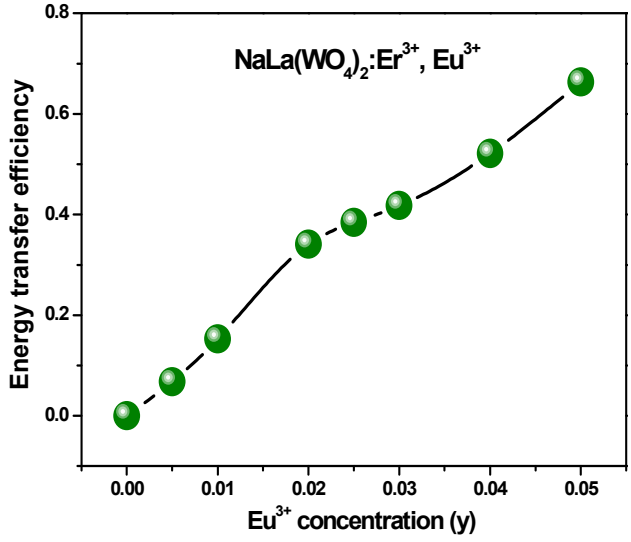

Fig. 9 Dependence of energy–transfer efficiency (η_T) on Eu^{3+} concentration for $NaLa(WO_4)_2$:Er^{3+}, Eu^{3+} phosphors

The energy-transfer efficiencies (η_T) from Er^{3+} to Eu^{3+} were calculated using the following formula[31]

$$\eta_T = 1 - I/I_0 \quad (4)$$

in which I and I_0 are the emission intensities for sensitizers (Er^{3+}) with and without the acceptors ions (Eu^{3+}). The energy transfer efficiency calculated as a function of Eu^{3+} concentrations is shown in Fig. 9. The efficiency η_T increases gradually and reaches approximatively 70% at x=0.05. Moreover, the critical distance R_{Er-Eu} of energy transfer from Er^{3+} to Eu^{3+} can be estimated by using the concentration-quenching method according the equation (2), but here, the critical concentration x_c is defined as the total concentration of Er^{3+} and Eu^{3+}, at which the luminescence intensity of Er^{3+} is half of that in the absence of Eu^{3+}, it is 0.068. Therefore, the critical distance (R_{Er-Eu}) of energy transfer is calculated to be about 13.24 Å. As the increase of Eu^{3+} concentration, the distance between Er^{3+} and Eu^{3+} becomes small enough (shorter than 13.24 Å), so the resonant energy transfer occurs: $^4S_{3/2}(Er^{3+}) + {}^7F_0(Eu^{3+}) \rightarrow {}^4I_{15/2}(Er^{3+}) + {}^5D_0(Eu^{3+})$; $^2H_{11/2}(Er^{3+}) + {}^7F_0(Eu^{3+}) \rightarrow {}^4I_{15/2}(Er^{3+}) + {}^5D_1(Eu^{3+})$; $^2H_{9/2}(Er^{3+}) + {}^7F_0(Eu^{3+}) \rightarrow {}^4I_{15/2}(Er^{3+}) + {}^5D_3(Eu^{3+})$.[14, 20] The possible energy transfer mechanism is shown in Fig 11.

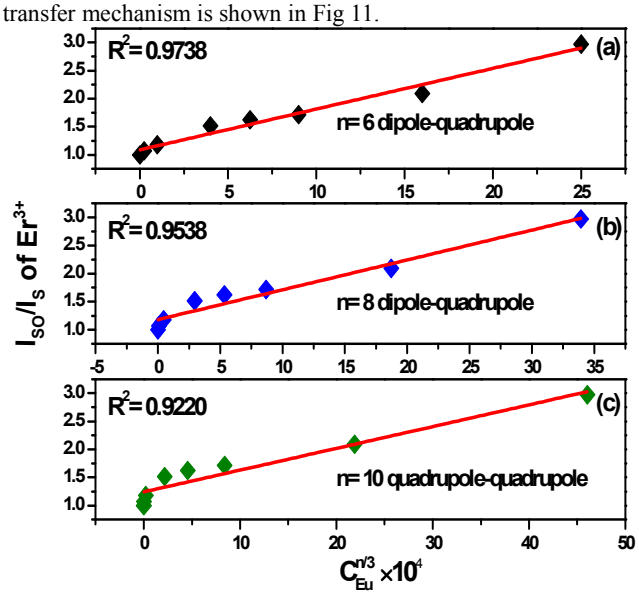

Fig. 10 The dependence I_{so}/I_s of Er^{3+} on the $C_{Eu}^{n/3} \times 10^4$ (n= 6, 8, 10) in $NaLa(WO_4)_2$:0.03Er^{3+},yEu^{3+} phosphors

In order to analyze the mechanism of energy-transfer process, we employ Dexter and Reisfeld's theory to deal with the luminescence intensities. The following equation can be used to analyze the potential mechanism [24, 32, 33]

$$I_{so}/I_s \propto C^{n/3} \quad (5)$$

where I_{so} is the intrinsic luminescence intensity of donors (Er^{3+}), and I_s is the luminescence intensity of donors in the presence of acceptors (Eu^{3+}); and C is the doped concentration of acceptors. When the value of n is 6, 8, or 10, the interaction corresponds to dipole-dipole, dipole-quadrupole, or quadrupole-quadrupole, respectively. The I_{so}/I_s plots are illustrated in Fig. 10, and the plots are used linear fitting. It can be clearly seen that when n= 6, linear fitting result is the best, clearly implying the predominate interaction mechanism for energy transfer process between Er^{3+} and Eu^{3+} ions in the $NaLa(WO_4)_2$ host is based on the dipole-dipole interactions.

A schematic model proposed for the probable ways of energy transfer in $NaLa(WO_4)_2$:Er^{3+},Eu^{3+} phosphors is shown in Fig. 11.

During the excitation process, the electrons situated at oxygen 2p states absorb energies of photons from UV. As consequence of this phenomenon, the energetic electrons are promoted to tungsten 5d states located near the conductor band[34]. When the electrons fall back to lower energy states again via blue emission and energy transfer to Er^{3+} and Eu^{3+} ions, and some energy is lost by cross relaxation. In addition, Er^{3+} ions sited in excited states such as $^4S_{3/2}$, $^2H_{11/2}$ and $^2H_{9/2}$ could transfer energy to Eu^{3+} ions sited in excited states such as ^5D_J (J=0,1,3) through phonon assisted dipolar-dipolar interaction[7,14,18,19,20], then relax to $^5D_0$ energy level, and finally transfer to the $^7F_1$ or $^7F_2$ level of Eu^{3+} ions by radiative transition.

The energy transfer among activator ions (Er^{3+}, Eu^{3+}) offers an approach to tune emission colors. Therefore, the CIE chromaticity coordinates for the phosphors excited at different wavelengths were determined based on their corresponding PL spectra, which are represented in the CIE diagram of Fig. 12 and the data is given in Tab. 1. $NaLa(WO_4)_2:Er^{3+}$ phosphor yields bluish green emission under 364 nm radiation, whereas that gives green light with excitation at 378 nm (Fig. 12, point a_1 and a_2). For the $NaLa(WO_4)_2:Er^{3+},Eu^{3+}$ phosphors, the Er^{3+} doping concentration is fixed at 0.03, as the concentration of Eu^{3+} increases from 0.005 to 0.05. It can be seen that when excited at 364 nm, the trend of the color tones changes from bluish green to pink through white with higher correlated color temperature. In addition, when excited by 378 nm those phosphors exhibit green emissions (point b_2, c_2, d_2 and e_2 in Fig. 12) and the color changes to white (point f_2, g_2 and h_2 in Fig. 12) and the correlated color temperature becomes low gradually by adjusting the doping concentration of Eu^{3+}, reflecting that the increasing of the Eu^{3+} concentration, the red component, could decrease the correlated color temperature at an exponential rate. Especially, there are two points at (0.356, 0.368) and (0.387, 0.364) with lower correlated color temperature of 4673, 3684 K, respectively, they will be potential on the application in WLEDs.

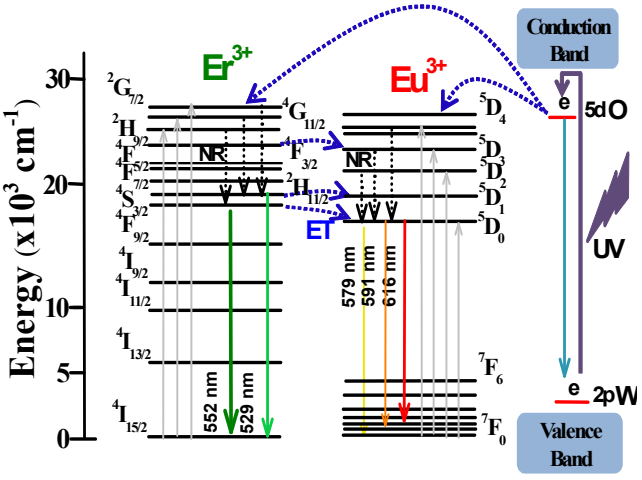

Fig. 11 Schematic energy–level diagram showing the excitation and emission mechanism of $NaLa(WO_4)_2:Er^{3+},Eu^{3+}$ phosphors (ET: energy transfer; NR: nonradiative)

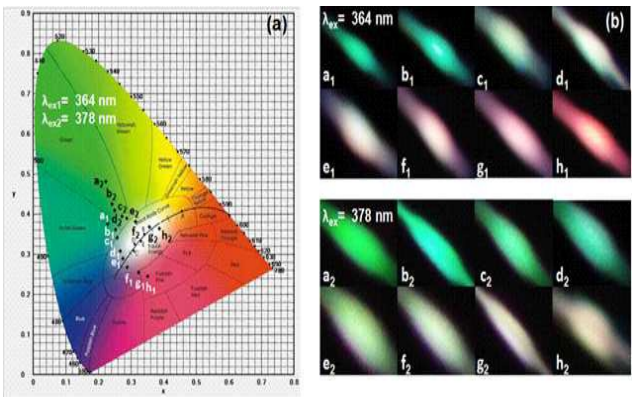

Fig. 12 CIE chromaticity diagram (a) and correlated color temperature (b) of the $NaLa(WO_4)_2:Er^{3+}$, Er^{3+} phosphors under different wavelengths excitation

Tab. 1 The CIE chromaticity coordinates for $NaLa(WO_4)_2:Er^{3+}$, Er^{3+} phosphors under different wavelengths excitation

Lab.	Samples $NaLa(WO_4)_2:Er^{3+}$, Er^{3+}	λ_{ex}= 364 nm CIE (x, y)	CCT /K	λ_{ex}= 378 nm CIE (x, y)	CCT /K
a	0.03Er	(0.228, 0.376)	10551	(0.223, 0.481)	8677
b	0.03Er, 0.005Eu	(0.252, 0.362)	9495	(0.241, 0.426)	8753
c	0.03Er, 0.01Eu	(0.258, 0.342)	9689	(0.249, 0.409)	8676
d	0.03Er, 0.02Eu	(0.267, 0.308)	10296	(0.272, 0.394)	7867
e	0.03Er, 0.025Eu	(0.274, 0.289)	10607	(0.287, 0.389)	7271
f	0.03Er, 0.03Eu	(0.288, 0.268)	10225	(0.314, 0.381)	6217
g	0.03Er, 0.04Eu	(0.323, 0.255)	6301	(0.356, 0.368)	4673
h	0.03Er, 0.05Eu	(0.351, 0.246)	3464	(0.387, 0.364)	3684

3.4 Up conversion luminescence properties and mechanism of $NaLa(WO_4)_2:Er^{3+},Eu^{3+}$ phosphors

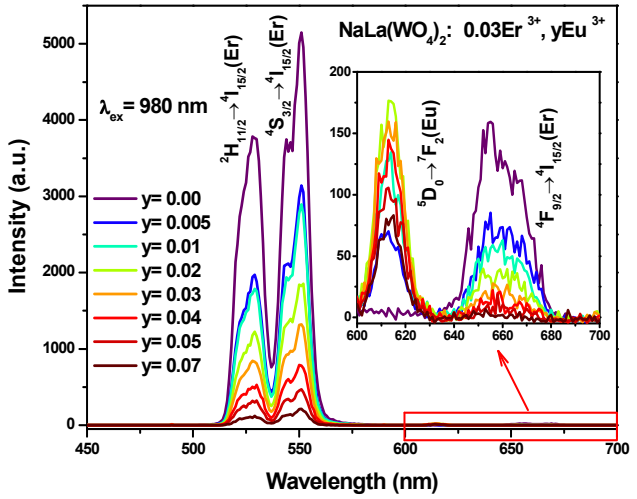

Fig. 13 UC luminescence spectra for $NaLa(WO_4)_2$: $0.03Er^{3+}$,yEu^{3+} phosphors (excited at 980 nm)

In view of Er^{3+} playing an indispensible role in UC luminescence, we study the UC luminescence properties and mechanism of the obtained codoped samples. Fig. 13 displays the UC luminescence spectra of $NaLa(WO_4)_2$:Er^{3+},Eu^{3+} under 980 nm excitation. From Fig. 13, it can be seen that the most emissions of Er^{3+} ions correspond well to what observed with 378 nm excitation, remarkably including a red emission of Er^{3+} assigned to $^4F_{9/2}\rightarrow{}^4I_{15/2}$ transitions at 655 nm exhibited in the enlarged inset of Fig. 13. In addition, it is significant that the UC of Eu^{3+} is obtained near 612 nm by the effect of the energy transfer between NIR absorbing Er^{3+} ions and Eu^{3+} emitters. As fixed the doping concentration of Er^{3+} at 0.03, with increasing Eu^{3+} concentration, the UC emission intensities of the Eu^{3+} first increase to an optimum concentration at 0.02 then decrease due to the concentration quenching, whereas that of the Er^{3+} decreases monotonically, reflecting the result of energy transfer from Er^{3+} to Eu^{3+}: $^4S_{3/2}(Er^{3+}) + {}^7F_0(Eu^{3+}) \rightarrow {}^4I_{15/2}(Er^{3+}) + {}^5D_0(Eu^{3+})$; $^2H_{11/2}(Er^{3+}) + {}^7F_0(Eu^{3+}) \rightarrow {}^4I_{15/2}(Er^{3+}) + {}^5D_1(Eu^{3+})$; $^2H_{9/2}(Er^{3+}) + {}^7F_0(Eu^{3+}) \rightarrow {}^4I_{15/2}(Er^{3+}) + {}^5D_3(Eu^{3+})$. Simultaneously, the low energy levels $^5D_{3,2,1,0}$ of Eu^{3+} ions could be populated through a series of nonradiative relaxations from the neighboring high excited levels.

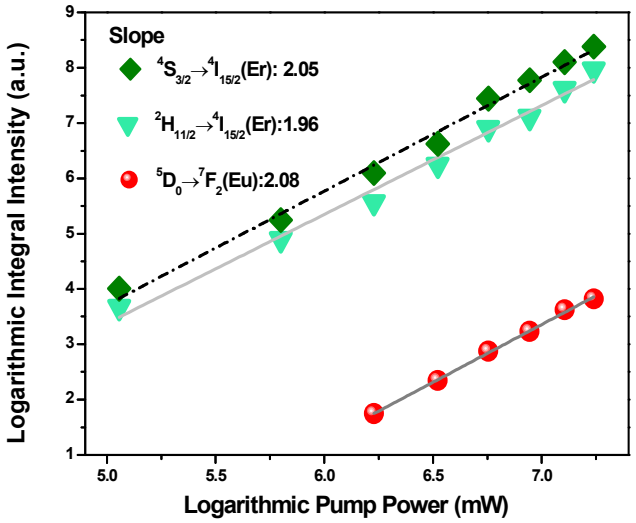

Fig. 14 Dependences of the logarithm of intensity on the logarithm of excitation power at 980 nm of $NaLa(WO_4)_2$: $0.03Er^{3+}$, $0.02Eu^{3+}$ phosphor

To understand the UC processes well, we investigated the excitation power at 980 nm dependence of the UC emission intensities. For an unsaturated UC process, the integrated UC luminescence intensity I is proportional to P^n [35, 36]

$$I \propto P^n \qquad (6)$$

where P is the pumping laser power, and n is the number of laser photons required in populating the upper emitting state. Fig. 14 shows the typical pump-power dependence of UC luminescence of $NaLa(WO_4)_2$:$0.03Er^{3+}$,$0.02Eu^{3+}$. The values of photon number n are 2.05 for the $^4S_{3/2}\rightarrow{}^4I_{15/2}$ transition of Er^{3+}, 1.96 for the $^2H_{11/2}\rightarrow{}^4I_{15/2}$ transition of Er^{3+}, 2.08 for the $^5D_0\rightarrow{}^7F_2$ transition of Eu^{3+}, indicating that all these transitions for Er^{3+} and Eu^{3+} ions are two-photon UC processes, respectively. The two-photon mechanism was also found previously in other Er^{3+} and Eu^{3+} ions codoped phosphors, such as that reported by Wang and Rai.[14, 20] Power dependence analyses illustrate that these levels of Eu^{3+} have the same multi-photon UC characters with the corresponding levels of Er^{3+} ions and confirm that they are populated by the energy transfer from the corresponding levels of Er^{3+}.

4 Conclusions

In summary, series novel color-tunable single-component $NaLa(WO_4)_2$: Er^{3+}, Eu^{3+} phosphors were prepared by one-step hydrothermal method at 180 ℃ for 20 h. For $NaLa(WO_4)_2$: Er^{3+} phosphors, Er^{3+} ions generate intense emission owing to the host sensitization effect. Under the excitation of ultraviolet, individual Er^{3+} ions activated $NaLa(WO_4)_2$ phosphors exhibit excellent bluish green or green emissions and the Er^{3+} ions quench at the concentration of 0.03 via a resonant type dipole-dipole interaction. In the case of Er^{3+} and Eu^{3+} co-doped systems, under the UV light excitation, the bright green emissions of Er^{3+} ions and the red characteristic emission of Eu^{3+}ions can be observed, the efficient energy transfer process between $Er^{3+} \rightarrow Eu^{3+}$ occurs via the dipole-dipole mechanism. Those single-component phosphors exhibit abundant color-tunable emissions besides warm white light with low correlated color temperature in the $NaLa(WO_4)_2$ host. Almost all of the prepared phosphors could find applications in WLEDs. More functionally, under 980 nm laser excitation, these phosphors also exhibit intense green and red emissions by the Er^{3+}–Eu^{3+} energy transfer process, which causes the observed UC of Eu^{3+}. The mechanisms of UC luminescence of both Er^{3+} and Eu^{3+} are determined to be two-photon UC processes.

Acknowledgements

This work was supported by the National Natural Science Foundation of P.R. China (NSFC) (Grant No. **51072026**, **51573023**) and the Development of Science and Technology Plan Projects of Jilin Province (Grant No. **20130206002GX**).

Notes and references

Key Laboratory of Applied Chemistry and Nanotechnology at Universities of Jilin Province, Changchun University of Science and Technology, Changchun, China. Fax: +86-431-85383815; Tel: +86-431-85582574; E-mail: liuguixia22@163.com

[1]S. Nakamura, T. Mukai and M. Senoh, *Appl. Phys. Lett.*, 1994, **64**, 1687−1689.
[2]Y. Jia, W. Lü, N. Guo, W. Lü, Q. Zhao and H. You, *Phys. Chem. Chem. Phys.*, 2013, **15**, 6057−6062.
[3]W. Lü, Y. Jia, W. Lv, Q. Zhao and H. You, *New J. Chem.*, 2013, **37**, 3701−3705.
[4]W. B. Im, S. Brinkley, J. Hu, A. Mikhailovsky, S. P. DenBaars and R. Seshadri, *Chem. Mater.*, 2010, **22**, 2842−2849.
[5]N. Guo, W. Lü, Y. Jia, W. Lv, Q. Zhao and H. You, *ChemPhysChem*, 2013, **14**, 192−197.
[6]W. Lü, N. Guo, Y. Jia, Q. Zhao, W. Lv, M. Jiao, B. Shao and H. You, *Inorg. Chem.*, 2013, **52**, 3007−3012.
[7]G. Seeta Rama Raju, E. Pavitra and J. S. Yu, *Dalton Trans.*, 2014, **43**, 9766−9776.
[8]Y. Liu, G. Liu, X. Dong, J. Wang and W. Yu, *RSC Adv.*, 2014, **4**, 58708–58716.
[9]D. Wen and J. Shi, *Dalton Trans.*, 2013, **42**, 16621−16629.
[10]Y. Liu, G. Liu, J. Wang, X. Dong and W. Yu, *Inorg. Chem.*, 2014, **53**, 11457−11466.

[11]X. Liu, W. Hou, X. Yang and J. Liang, *CrystEngComm*, 2014, **16**, 1268−1276.
[12]N. S. Singh, N. K. Sahu and D. Bahadur, *J. Mater. Chem. C,* 2014, **2**, 548−555.
[13]M. Shang, D. Geng, X. Kang, D. Yang, Y. Zhang and J. Lin, *Inorg. Chem.*, 2012, **51**, 11106−11116.
[14]L. Wang, X. Xue, H. Chen, D. Zhao and W. Qin, *Chem. Phys. Lett.,* 2010, **485**, 183–186.
[15]D. Kasprowicz, M.G. Brik, A. Majchrowski, E. Michalski and P. Głuchowski, *J. Alloys Compd.,* 2013, **577**, 687–692.
[16]R. Krishnan and J. Thirumalai, *New J. Chem*., 2014, **38**, 3480−3491.
[17]X. Mateos, M.C. Pujol, F. Guell, R. Sole, Jna Gavalda, J. Massons, M. Aguilo and F. Diaz, *Opt. Mater.*, 2004, **27**, 475–479.
[18]Y. Dwivedi, A. Rai, and S. B. Rai, *J. Lumin.,* 2009, **129**, 629.
[19]J. Sun, W. Zhang, W. Zhang, and H. Du, *Mater. Res. Bull*., 2012, **47**, 786.
[20]V. K. Rai, A. Pandey, and R. Dey, *J. Appl. Phys.*, 2013, **113**, 083104-083106.
[21] X. Liu, W. Hou, X. Yang and J. Liang, *CrystEngComm*, 2014, **16**, 1268-1276.
[22] S. Huang, D. Wang, C. Li, L. Wang, X. Zhang, Y. Wan and P. Yang, *CrystEngComm*, 2012, **14**, 2235-2244.
[23]G. Blasse and B. C. Grabmaier, inLuminescent Materials, Springer Berlin Heidelberg, 1994, p. 71.
[24]S. A. Yan, J. W. Wang, Y. S. Chang, W. S. Hwang and Y. H. Chang, *Opt. Mater.*, 2011, **34**, 147–151.
[25]G. Blasse, *Philips Res. Rep.*1969, **24**, 131−144.
[26]N. Guo, H. You, Y. Song, M. Yang, K. Liu, Y. Zheng, Y. Huang and H. Zhang, *J. Mater. Chem.,* 2010, **20**, 9061–9067.
[27]L. G. Van Uitert, *J. Electrochem. Soc.,* 1967, **114**, 1048–1053.
[28]Z. Xia, R. S. Liu, K. W. Huang and V. Drozd, *J. Mater. Chem.,* 2012,**22**, 15183–15189.
[29]Z. Xia, Y. Zhang, M. S. Molokeev and V. V. Atuchin, *J. Phys. Chem. C*, 2013, **117**, 20847–20854.
[30]J. Lin, Q. Su, S. Wang and H. Zhang, *J. Mater. Chem.,* 1996, **6**, 265−269.
[31]C. Y. Cao, H. K. Yang, J. W. Chuang, B. K. Moon, B. C. Choi, J. H. Jeong and K. H. Kim, *J. Mater. Chem.,* 2011, **21**, 10342−10347.
[32]D. L. Dexter and J. H. Schulman, *J. Chem. Phys.,* 1954, **22**, 1063–1070.
[33]R. Reisfeld, E. Greenberg, R. Velapoldi and B. Barnett, *J. Chem. Phys.*, 1972, **56**, 1698–1705.
[34]J. C. Sczancoski, L. S. Cavalcante, N. L. Marana, R. O. Silva, R. L. Tranquilin, M. R. Joya, P. S. Pizani, J. A. Varela, J. R. Sambrano, M. Siu Li, E. Longo and J. Andr´es,*Curr, Appl. Phys.,* 2010, **10**, 614–624.
[35]R. Scheps, *Ptog. Quant. Electron*., 1996, **20**, 271–358.
[36]T. Grzyb, A. Gruszeczka, R. J. Wiglusz and S. Lis, *J. Mater. Chem. C,* 2013, **1**, 5410–5418.